Optical sources of non-linearity in heterodyne interferometers

A. E. Rosenbluth and N. Bobroff*

Non-linearity of the two-frequency Michelson interferometer is studied by measurement of the modulation in phase and amplitude of the interference signal at the receiver. An important conclusion is that frequency mixing is not a major cause of non-linearity unless the mixing is asymmetric between the two arms of the interferometer. One source of asymmetry is non-orthogonality of the frequency states produced by the laser. Differential transmission between the reference and measurement paths can cause polarization states that are initially orthogonal to become non-orthogonal at the interferometer output. The influence of beam-splitter leakage, misorientation of the polarization axes of the source, and imperfect waveplates are also considered. It is not widely known that typical retroreflectors cause about a 7° rotation of the polarization state. However, polarization mixing induced by the retroreflectors is small in most, but not all, common configurations of the interferometer.

Keywords: *interferometry, non-linearities, frequency mixing, polarization mixing*

Polarization mixing between the two interfering optical frequencies in a heterodyne interferometer causes a non-linear relation between the actual and measured phase[1-4]. The non-linearity, which can be as large as 10 nm, is an important consideration in measurement applications requiring nanometre accuracy if the measurement range exceeds about one half of a fringe. In the first section of this paper, a technique for experimental study of the non-linearity based on observation of the amplitude modulation of the beat signal at the receiver is presented. Next, the following sources of frequency mixing are investigated: (1) misalignment of the laser polarization axes to those of the polarizing beam-splitter, (2) ellipticity of the light source, (3) differential transmission between the two arms of the interferometer, (4) rotation of polarization by the retroreflectors, (5) leakage through the beam-splitter, and (6) waveplate errors.

The heterodyne Michelson interferometer

A typical configuration for the interferometer is shown in Fig 1. Two different optical frequencies f_1 and f_2 enter the interferometer with polarization states that are nominally orthogonal. The f_1 and f_2 beams are then directed by a polarizing beam-splitter into the measurement and reference arms, respectively. The complex amplitude of frequency state f_1 is A, and is B for f_2.

Specific sources of optical mixing are considered below. Initially, we treat such mixing by

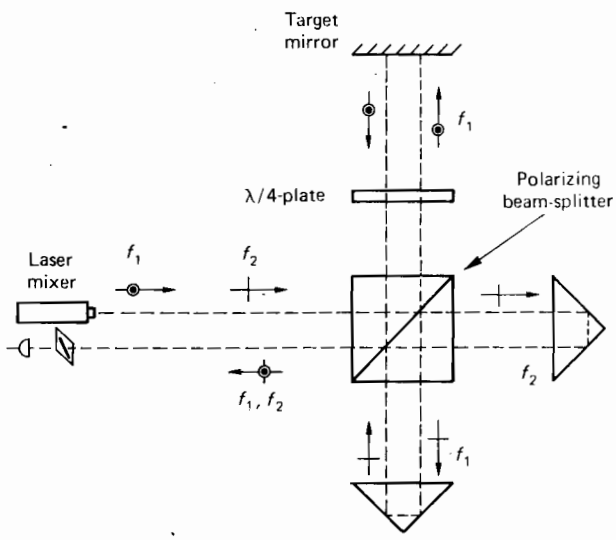

Fig 1 Typical configuration of the heterodyne Michelson interferometer

assuming that the nominal amplitudes A and B are 'contaminated' by complex amplitudes β and α that have the wrong phase. The mixing mechanisms described below give rise to an amplitude α at frequency f_1 that essentially follows the reference optical path taken by amplitude B (frequency f_2), and also to an amplitude β at f_2 that essentially follows the nominal f_1 path of amplitude A. Such mixing causes periodic non-linearity at the fundamental harmonic of the interferometer (period of one fringe). Non-linearities that involve more general mixing paths will be described in a later publication[5].

* *IBM Thomas J Watson Research Center, PO Box 218, Yorktown Heights, New York 10598, USA*

 0141-6359/90/010007-05

The measurement arm states are Doppler shifted, recombined with the reference beam, and subsequently mixed and imaged on a photodiode detector. This results in an electric field E at the photodetector proportional to

$$E \propto Ae^{2\pi if_1} + \alpha e^{2\pi if_1} + Be^{2\pi if_2} + \beta e^{2\pi if'_2}$$

where the primed frequencies denote a Doppler shift. The receiver signal resulting from $|E^2|$ has four components:

1. A constant dc offset given by

$$|A|^2 + |B|^2 + |\alpha|^2 + |\beta|^2$$

2. Homodyne modulation (essentially Michelson intensity fringes, assumed near-dc),

$$2|B||\beta|\cos(\Phi_B - \Phi_\beta) + 2|A||\alpha|\cos(\Phi_\alpha - \Phi_A)$$

3. The basic heterodyne measurement contribution at beat frequency $\Delta f \equiv f_1 - f_2$;

$$2|A||B|\cos(2\pi\Delta ft + \Phi_A - \Phi_B),$$

with Φ_B the constant phase of the reference amplitude B, and Φ_A the integrated Doppler shift produced by motion of the measurement arm mirror,

4. Undesired mixing terms at Δf that cause a non-linear position error,

$$2|B||\alpha|\cos(2\pi\Delta ft + \Phi_\alpha - \Phi_B) + 2|A||\beta|\cos(2\pi\Delta ft + \Phi_A - \Phi_\beta) + 2|\alpha||\beta|\cos(2\pi\Delta ft + \Phi_\alpha - \Phi_\beta)$$

A high pass filter is used to couple the receiver output to the phase measurement system, removing the offset and homodyne components. The filtered signal, S, is

$$S \propto \cos(2\pi\Delta ft + \Phi_A - \Phi_B) + \frac{|\alpha|}{|A|}\cos(2\pi\Delta ft + \Phi_\alpha - \Phi_B) + \frac{|\beta|}{|B|}\cos(2\pi\Delta ft + \Phi_A - \Phi_\beta) + \frac{|\alpha|}{|A|}\frac{|\beta|}{|B|}\cos(2\pi\Delta ft + \Phi_\alpha - \Phi_\beta) \quad (1)$$

The first term of Eq 1 is the nominal beat signal, whose phase, $\Phi_M \equiv \Phi_A - \Phi_B$, is proportional to the difference in path length between the measurement and reference arms. To understand how the remaining three terms in Eq (1) influence the measurement of Φ_M, note that an expression of the form $\cos(2\pi\Delta ft + \Phi)$ can be expanded into quadratures, ie $(\cos\Phi)\cos(2\pi\Delta ft) + (-\sin\Phi)\sin(2\pi\Delta ft)$. Association of each quadrature $\cos(2\pi\Delta ft)$ and $\sin(2\pi\Delta ft)$ with the $\tilde{x}$ and $\tilde{y}$ axes of a Cartesian coordinate system produces a vector analogue of each cosinusoidal oscillation, as depicted in the phasor diagram of Fig 2a. The phasor representation of Eq 1 has the polar

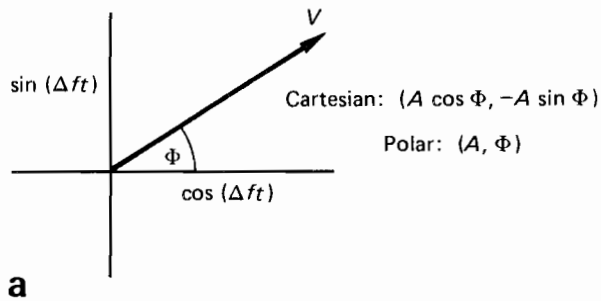

a

Fig 2 (a) Phasor representation of heterodyne signal

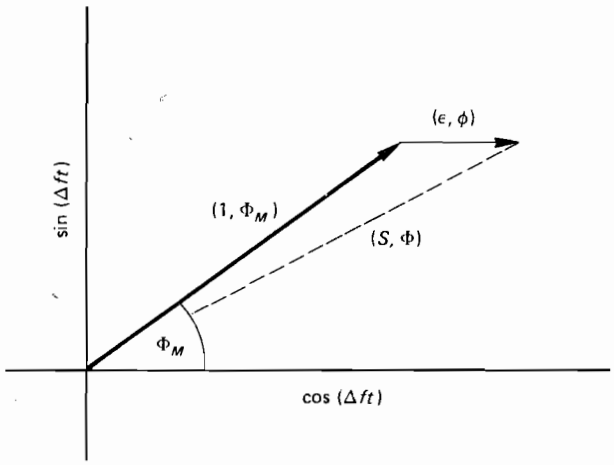

(1, Φ_M): amplitude and phase of ideal signal
(ϵ, ϕ): amplitude and phase of the mixing vector
(S, Φ) = (1- δS, $\Phi_M - \delta\Phi$) measured amplitude, phase

b

Fig 2 (b) First-order phasor diagram of non-linearity

(magnitude, phase) form

$$(S, \Phi) = (1, \Phi_M) + \left(\frac{|\alpha|}{|A|}, \Phi_\alpha - \Phi_B\right) + \left(\frac{|\beta|}{|B|}, \Phi_A - \Phi_\beta\right) + \left(\frac{|\alpha|}{|A|}\frac{|\beta|}{|B|}, \Phi_\alpha - \Phi_\beta\right) \quad (2)$$

The first term on the right represents the basic measurement signal, which rotates about the origin with Φ_M. The terms of first order in α and β represent optical frequency mixing at fixed phase (phasor angle), since α and B, as well as β and A, are assumed in Eq (1) to travel a common path. The first order mixing terms then form the constant phasor

$$(\epsilon, \phi_\epsilon) \equiv \left(\frac{|\alpha|}{|A|}, \Phi_\alpha - \Phi_\beta\right) + \left(\frac{|\beta|}{|B|}, \Phi_A - \Phi_\beta\right)$$

The final term in Eq (2) is interesting in that it rotates in the opposite sense as the basic measurement phase Φ_M. This causes a second-order non-linearity at the second harmonic of the interferometer[5].

Fig 2b shows the phasor Eq (2) to first order in the mixing. The phase of the resultant, Φ, differs from Φ_M by a measurement error $\delta\Phi_M$. The measured phase lags and leads the true phase as the $(1, \Phi_M)$ vector rotates about the origin. It is clear from Fig 2b that the magnitude S of the resultant vector also varies with Φ_M. To first order, the amplitude modulation δS and phase modulation $\delta\Phi_M$ lie on a circle of radius ε, so that

$$\delta S^2 + \delta\Phi_M^2 = \varepsilon^2 \qquad (3)$$

The amplitude modulation is represented by the sinusoidal projection of the fixed mixing phasor in the direction of the rotating phasor of the ideal signal. The phase error is represented by the cosinusoidal projection of the mixing phasor in the direction perpendicular to the ideal signal phasor.

Fig 3 shows an experimental observation of these relationships[4]. The vertical axis is the phase difference between two independent interferometers configured to measure the distance to a common mirror. The horizontal axis is displacement (1 fringe full scale). The non-linearity is seen to have the predicted sinusoidal dependence on displacement.

If this trace is superimposed on the amplitude modulation signal taken from the test point output of the receiver, each zero crossing of the phase error is observed to occur at an extremum of the amplitude modulation, verifying the quadrature relationship of Eq (3). The first-order relation between δS and $\delta\Phi_M$ can be more complicated when non-linearity occurs from mixing paths that arise internally in the interferometer as a consequence of errors in the interferometer components[5].

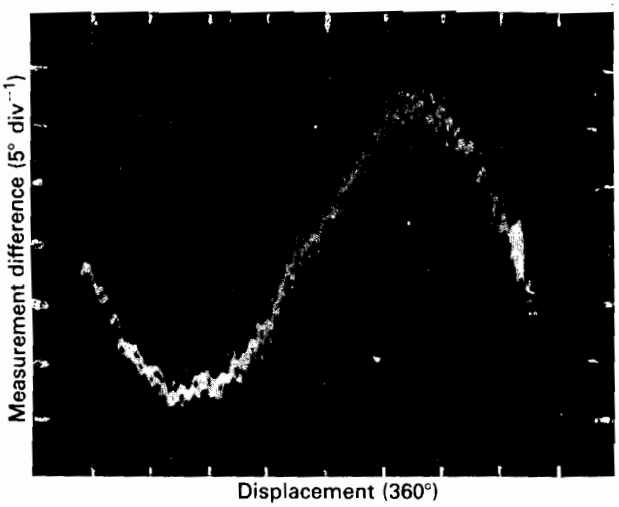

Fig 3 Sinusoidal oscillation of the phase non-linearity (from Ref 4). The vertical scale is the phase difference between two independent interferometers monitoring a common mirror. A $\lambda/2$-plate and differential transmission are used to generate significantly more non-linearity in one interferometer than the other. The horizontal axis is displacement. See Ref 4 for further details on the experimental system

The functional relation Eq (3) can be exploited to make *in situ* studies of $\delta\Phi_M$ by measuring δS. A simple technique for the study of the interferometer signal is to observe directly the output at the receiver photodiode. This is readily accomplished with most commercial receivers by attaching a low impedance coaxial cable to the output of the first preamplifier stage following the diode. The signal is coupled to an oscilloscope by a high pass RC filter having a single pole at 10 kHz. In our experiments the filter removes both constant and homodyne terms from the signal. Fig 4 shows a typical beat signal from an interferometer as the measurement mirror is slowly scanned. The signal shows an amplitude modulation δS of $\pm 10\%$. Since Eq (3), linking the phase modulation $\delta\Phi_M$ to the amplitude modulation δS, is the equation of a circle, we conclude that the radius E in phasor space is 0.10, and that the signal contains a phase modulation $\delta\Phi_n$ amounting to ± 0.10 rad. This is a displacement error of about $\lambda/128$ for a linear interferometer, and $\lambda/256$ for the plane mirror configuration. Because amplitude can be measured to very high accuracy, the technique is sensitive to non-linearities on the Angstrom scale.

Optical sources of frequency mixing

Efforts to account quantitatively for measured non-linearity quickly reveal the inadequacy of a purely scalar treatment. When polarization effects are included, a surprising result is that many commonly cited causes of frequency mixing are not in themselves sufficient to produce significant non-linearity, ie non-linearity proportional to the first power of improperly polarized amplitudes like α and β above.

An example that illustrates this is misorientation of the laser polarization axes relative to those of the beam-splitter. This might result from improper

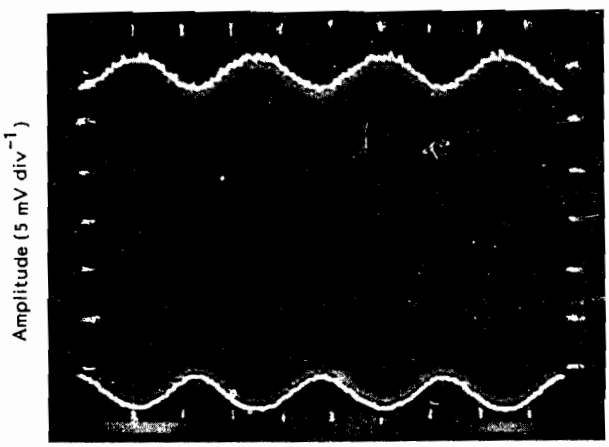

Fig 4 Nonlinearity in the y-axis servo of an electron-beam lithography tool. As the stage is scanned back and forth, the beat signal amplitude varies through a range of about 20% from sweep to sweep. The $\pm 10\%$ amplitude modulation indicates the presence of positional error amounting to $\pm 0.1/2\pi$ fringes

orientation of a $\lambda/4$-plate used to linearize the nominally circular Zeeman polarizations. If the laser axes are misaligned to the $\tilde{x}$ and $\tilde{y}$ axes of the beam-splitter by an angle Θ, the two frequency states entering the interferometer become

$$\tilde{E}_1 = |E_1| e^{2\pi i f_1} (\cos\Theta \tilde{y} + \sin\Theta \tilde{x})$$

$$\tilde{E}_2 = |E_2| e^{2\pi i f_2} (-\sin\Theta \tilde{y} + \cos\Theta \tilde{x})$$

Referring to Fig 1 and the discussion of the previous section, the complex amplitudes in the measurement arm ($\tilde{y}$ axis) are given by $A = |E_1| \cos\Theta e^{i\Phi_M}$, $\beta = |E_2| \sin\Theta e^{i\pi + \Phi_M}$, while those in the reference arm ($\tilde{x}$ axis) are $B = |E_2|(1-\varepsilon)\cos\Theta$, $\alpha = |E_1|(1-\varepsilon)\sin\Theta$. The factor $(1-\varepsilon)$is introduced to account for a difference in transmission between the measurement and reference arms. The interferometer optics are otherwise treated as ideal.

The vector output of the interferometer corresponding to Eq (2) is

$$(S, \Phi) = (1, \Phi_M) + ((1-\varepsilon)\tan\Theta, 0) + \left(\frac{\tan\Theta}{1-\varepsilon}, -\pi\right) + (\tan^2\Theta, -\pi - \Phi_M) \quad (4)$$

Note that the mixing terms of order Θ are 180° out of phase, and would cancel if $\varepsilon = 0$. The phase error $\delta\Phi = \Phi - \Phi_M$ resulting from (4) is

$$\delta\Phi = 2\varepsilon \tan\Theta \sin\Theta_M - \tan^2\Theta \sin 2\Phi_M$$

and the amplitude modulation is

$$\delta S = 1 - 2\varepsilon \tan\Theta \cos\Phi_M + \tan^2\Theta \cos 2\Phi_M$$

For small ε, rotational misalignments do not cause a significant non-linearity, despite the introduction of substantial optical mixing. The frequencies are in orthogonal polarization states that do not interfere, despite overlap along the $\tilde{x}$ and $\tilde{y}$ axes. Thus, each arm of the interferometer gives rise to a beat signal corresponding to the presence of both frequencies in the arm, but the beat signals for the two arms are 180° out of phase with each another. An experimental demonstration is shown in Fig 5.

In real systems the coherent transmittance can depart significantly from 1, particularly in multi-pass systems[6]. Differential transmittance essentially causes polarization states that are initially orthogonal at the input to become coupled at the output, giving rise to substantial non-linearity. In systems we have examined, this is often the largest source of non-linearity.

Another important source of optical mixing is non-orthogonality of the elliptical polarizations of the frequency states produced by the laser head. As shown in Fig 6, non-orthogonality can involve either unequal eccentricity or non-perpendicular orientation of the ellipses. Assuming for simplicity that the f_1 polarization has major axis along $\tilde{y}$, the frequency states entering the interferometer are

$$\tilde{E}_1 = |E_1| e^{2\pi i f_1} (\tilde{y} + e_1 e^{-i(\pi/2)} \tilde{x})$$

$$\tilde{E}_2 = |E_2| e^{2\pi i f_2} [(e_2 \cos\Theta e^{-i(\pi/2)} + \sin\Theta)\tilde{y} + (-e_2 \sin\Theta e^{-i(\pi/2)} + \cos\Theta)\tilde{x}]$$

The complex amplitudes in the measurement

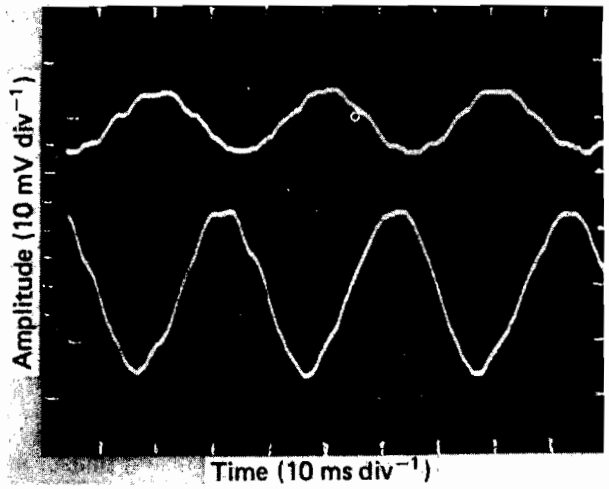

Fig 5 Mixing due to orientation error. One arm at a time is blocked while a $\lambda/2$ plate rotates the polarization axes at the interferometer input. The non-zero beat signals in the open arms indicate the presence of frequency mixing, but the contributions from the two arms are 180° out of phase, The coherent transmittance of the beat signal is smaller in the measurement arm than in the reference arm, hence the system shows significant net non-linearity

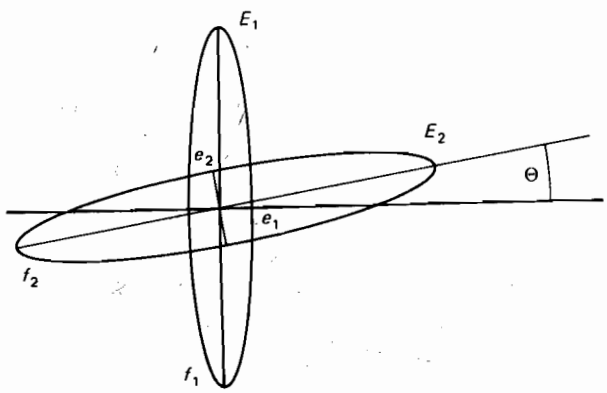

Fig 6 Elliptical or rotated inputs do not cause first order non-linearity if the polarizations are orthogonal, ie non-interfering. Orthogonality requires ellipticities that are equal and opposite, as well as perpendicular orientation

arm ($\tilde{y}$ axis) are given by

$$A = |E_1| e^{i\Phi_M},$$

$$\beta = |E_2| e^{i\Phi_M} (e_2 \cos\Theta e^{-i(\pi/2)} + \sin\Theta)$$

while those in the reference ($\tilde{x}$ axis) are

$$B = |E_2| (-e_2 \sin\Theta e^{-i(\pi/2)} + \cos\Theta)$$

$$\alpha = |E_1| e_1 e^{-i(\pi/2)}$$

Some algebraic gymnastics lead to the vector equivalent of Eq (2)

$$(S, \Phi) = (1, \Phi_M) + \left((\tan^2\Theta + e_2^2)^{1/2}, \tan^{-1}\left(\frac{-e_2}{\tan\Theta}\right)\right) + \left(e_1, \frac{\pi}{2}\right)$$

The phase error is

$$\delta S = -(e_1 - e_2) \sin \Phi_M + \tan \Theta \cos \Phi_M.$$

and the amplitude error is

$$\delta S = -(e_1 - e_2) \sin \Phi_M + \tan \Theta \cos \Phi_M.$$

For $\Theta = 0$, the ellipses are orientated at 90° and the first order mixing vectors point in opposite directions. For equal eccentricities ($e_1 = e_2$), the first order non-linearity vanishes despite the presence of frequency mixing.

Eccentricity and misorientation of frequency states are important sources of non-linearity with older laser heads. We have seen eccentricities as high as 0.1 and Θ as large as 3°. For the case $e_1 = e_2$, $\Theta_1 = \Theta_2$, unequal transmission of the reference and measurement arms can introduce an indirect non-linearity. A direct non-linearity, typically somewhat smaller, is produced when $e_1 \neq e_2$, $\Theta_1 \neq \Theta_2$. Many laser heads of more recent vintage show orientation and eccentricity errors below 0.015, but eccentricities at 0.04 are sometimes seen. Further details are provided in Ref 5.

Rotational misalignment and ellipticity are sources of frequency mixing which occur prior to introduction of light into the interferometer proper. Several sources of frequency mixing exist in the optics of the interferometer. These effects are considered next.

It is not widely recognized that the retroreflectors cause a substantial rotation of the plane of polarization of the incident light, and introduce a small ellipticity. These optical elements are typically figured from solid glass and coated with silver to obtain a high reflection efficiency. Using standard methods (eg Ref 7), the primary effect is found to be a rotation of the plane of polarization by about 7°. This does not introduce a first order non-linearity in most configurations of the interferometer, because the beams are substantially repolarized by a second passage through the polarizing beam-splitter. However, polarization rotation by retroreflectors can open first-order mixing paths in certain interferometer configurations described in the literature[5].

Another source of frequency mixing is leakage of the states at the polarizing beam-splitter. The rejection ratio of the beam-splitters is typically ~0.25% in intensity. Thus, the amplitude of the leakage can be ~5%. However, the leakage flux retains its polarization, and must pass through the beam-splitter at least once more before being mixed at the receiver. Thus, non-linearity caused by beam-splitter leakage is usually of second order in the amplitude leakage coefficient. Exceptional cases are described in Ref 5.

Similar conclusions apply to frequency mixing by faulty $\lambda/4$-plates. We have seen errors of order 10% in thickness and mounting orientation for these components; however, in all interferometers we have studied, the associated non-linearities are either proportional to the square or higher power of these errors, or require the presence of other errors in the system.

Acknowledgement

The authors would like to gratefully acknowledge the technical assistance of Douglas Golding at the University of Rochester, USA.

References

1 **Quenelle, R. C.** Nonlinearity in Interferometer Measurements, *Hewlett-Packard J 1983,* **34,** *10*
2 **Fedotova, G. V.** Analysis of the measurement error of the parameters of mechanical vibration, *Meas Techniques 1980,* **23,** *577–80*
3 **Sutton, C. M.** Non-linearity in length measurement using heterodyne laser Michelson interferometry, *J Phys E, 1987,* **10,** *1290–1292*
4 **Bobroff, N.** Residual Errors in Laser Interferometry from air turbulence and Nonlinearity, *Appl Opt, 1987,* **26,** *2676–2681*
5 **Rosenbluth, A. E. and Bobroff, N.** in preparation
6 **Baldwin, R. R. and Siddall, G. J.** 'A Double Pass Attachment for the Linear and Plane Mirror Interferometer, *Proc SPIE, 1984,* **480,** *78*
7 **Lamekin, P. I.** Polarization Properties of Corner Reflectors, *Sov J Opt Technol, 1988,* **55** *(1), 16–19*